JOURNAL
OF
THE ROYAL
SOCIETY

Interface

Leaf surface structures enable the endemic Namib desert grass Stipagrostis sabulicola to irrigate itself with fog water

A. Roth-Nebelsick, M. Ebner, T. Miranda, V. Gottschalk, D. Voigt, S. Gorb, T. Stegmaier, J. Sarsour, M. Linke and W. Konrad

Supplementary data	"Data Supplement" http://rsif.royalsocietypublishing.org/content/suppl/2012/02/16/rsif.2011.0847.DC1.html
References	**This article cites 32 articles, 3 of which can be accessed free** http://rsif.royalsocietypublishing.org/content/early/2012/02/15/rsif.2011.0847.full.html#ref-list-1 **Article cited in:** http://rsif.royalsocietypublishing.org/content/early/2012/02/15/rsif.2011.0847.full.html#related-urls
P<P	Published online 22 February 2012 in advance of the print journal.
Subject collections	Articles on similar topics can be found in the following collections biomaterials (186 articles) biomimetics (77 articles) environmental science (79 articles)
Email alerting service	Receive free email alerts when new articles cite this article - sign up in the box at the top right-hand corner of the article or click **here**

Advance online articles have been peer reviewed and accepted for publication but have not yet appeared in the paper journal (edited, typeset versions may be posted when available prior to final publication). Advance online articles are citable and establish publication priority; they are indexed by PubMed from initial publication. Citations to Advance online articles must include the digital object identifier (DOIs) and date of initial publication.

Leaf surface structures enable the endemic Namib desert grass *Stipagrostis sabulicola* to irrigate itself with fog water

A. Roth-Nebelsick[1],*, M. Ebner[2], T. Miranda[2], V. Gottschalk[4], D. Voigt[3], S. Gorb[3], T. Stegmaier[4], J. Sarsour[4], M. Linke[4] and W. Konrad[2]

[1]*State Museum of Natural History, Rosenstein 1, 70191 Stuttgart, Germany*
[2]*Department of Geosciences, University of Tübingen, Sigwartstrasse 10, 72076 Tübingen, Germany*
[3]*Zoological Institute, University of Kiel, Am Botanischen Garten 1-9, 24098 Kiel, Germany*
[4]*Institut für Textil- und Verfahrenstechnik Denkendorf, Körschtalstraße 26, 73770 Denkendorf, Germany*

The Namib grass *Stipagrostis sabulicola* relies, to a large degree, upon fog for its water supply and is able to guide collected water towards the plant base. This directed irrigation of the plant base allows an efficient and rapid uptake of the fog water by the shallow roots. In this contribution, the mechanisms for this directed water flow are analysed. *Stipagrostis sabulicola* has a highly irregular surface. Advancing contact angle is $98° \pm 5°$ and the receding angle is $56° \pm 9°$, with a mean of both values of approximately $77°$. The surface is thus not hydrophobic, shows a substantial contact angle hysteresis and therefore, allows the development of pinned drops of a substantial size. The key factor for the water conduction is the presence of grooves within the leaf surface that run parallel to the long axis of the plant. These grooves provide a guided downslide of drops that have exceeded the maximum size for attachment. It also leads to a minimum of inefficient drop scattering around the plant. The combination of these surface traits together with the tall and upright stature of *S. sabulicola* contributes to a highly efficient natural fog-collecting system that enables this species to thrive in a hyperarid environment.

Keywords: contact angle; surface grooves; directional water flow; surface roughness; fog collection; *Stipagrostis sabulicola*

1. INTRODUCTION

Wetting properties are important for many biological processes as well as for technical applications. A wide variation of wetting effects can be obtained by combining surface chemistry and surface structures [1]. Plant surfaces represent a group of biological surfaces that recently have generated much interest the Lotus effect leading to highly water repellent leaves as an example [2,3]. The underlying benefits of wetting effects on plant surfaces are manifold ranging from preventing pathogens from settling (as proposed for many water-repellent leaves), to ensuring the floating ability of aquatic plants [4] or to facilitating the catching of prey by carnivorous plants [5].

Wetting properties are also involved in the interactions between plants and dew or fog [6]. In many regions of the world, fog and dew represent regularly occurring phenomena, and the impact of these events on hydrology and ecology of the local vegetation is often substantial [7–9]. For example, fog drip (the shedding of droplets from leaves to the ground) and stem flow (the running-off of water from plant stems) may alter the local hydrological conditions [10–12]. In various arid regions, fog represents a valuable water source for the plants. This applies particularly for deserts with regular fog events, such as the hyperarid Namib Desert of South Western Africa [13]. Here, many organisms are adapted to use fog [14]. As fog collection has attained increasing interest during the last years as a sustainable water source in arid environments, a better understanding of the strategies that are employed by fog-harvesting organisms is expected to contribute to further improve the already existing technical fog collectors and fog-collecting strategies.

There is evidence that *Stipagrostis sabulicola*, a grass species endemic to the sand dunes of the Namib,

*Author for correspondence (anita.rothnebelsick@smns-bw.de).

depends to a large degree on fog collection ([15,16] and citations therein). This species is able to extract substantial quantities of water from fog with collection rates of $4-5 \, \text{mm}^3 \, \text{mm}^{-2}$ of leaf surface and fog event as was shown by measurements in the field [15,16]. During these fog events, intense droplet formation can be observed on the plant which consists of stiff culms with heights of up to 2 m. The scattering of droplets is quite rare despite the sagging of the upper parts of the culms. It can be observed in the field that droplets cling to the plant, coalesce with other droplets and then, after reaching a maximum size, glide downwards towards the roots. The collected water is mostly conducted towards the culm base. It becomes available for the roots and a fog event can be optimally exploited [16].

This study investigates how *S. sabulicola* achieves directed water conduction and prevents droplet-scattering during fog events. The results are compared with droplet behaviour on industrial fibres containing longitudinal ridges.

2. MATERIAL AND METHODS

2.1. Plant material

All studies were conducted with fresh or dry plant material from its original habitat. Plant material was collected close to the Gobabeb Research Station, located within the Naukluft National Park, Namibia (http://www.gobabebtrc.org/). The surface exposed to the fog is preferentially that of the abaxial leaf side (i.e. lower leaf side). The leaf basis is attached to the culm and the leaf lamina is involute in such a way that the abaxial side is directed outwards and the adaxial side (i.e. upper leaf side) is directed inwards (figure 1*a*,*b*). The plants were used untreated (i.e. not washed) to conserve the initial condition that prevailed at their growing site.

The culm of *S. sabulicola* has a thickness of about 5 mm at the base and tapers into a barbed tip (figure 1*a*,*b*). Preliminary studies showed that the surface characteristics of dry and fresh plants do not differ. This is mainly because of the very stiff character of the plant, which additionally shows pricking tips. These properties are achieved by a thick cuticle and substantial amounts of sclerenchyma [17].

2.2. Scanning electron microscopy analysis of the surface

The surface structure was studied using scanning electron microscopy (SEM), with a LEO Model 1450 VP (Variable Pressure; LEO Electron Microscopy Ltd, Clifton Road, UK) available at the Institute for Geosciences, University of Tübingen. Dry material was used for SEM. After mounting on stubs, the leaf pieces were sputtered with gold (15 nm) using a BAL-TEC Model SCD 005/CEA 035 (BAL-TEC GmbH, Witten, Germany). The specimen was observed under vacuum, with an accelerating voltage of 10 kV and a working distance of 15 mm. Additionally, the roughness of the surface was evaluated by using atomic force microscopy (AFM).
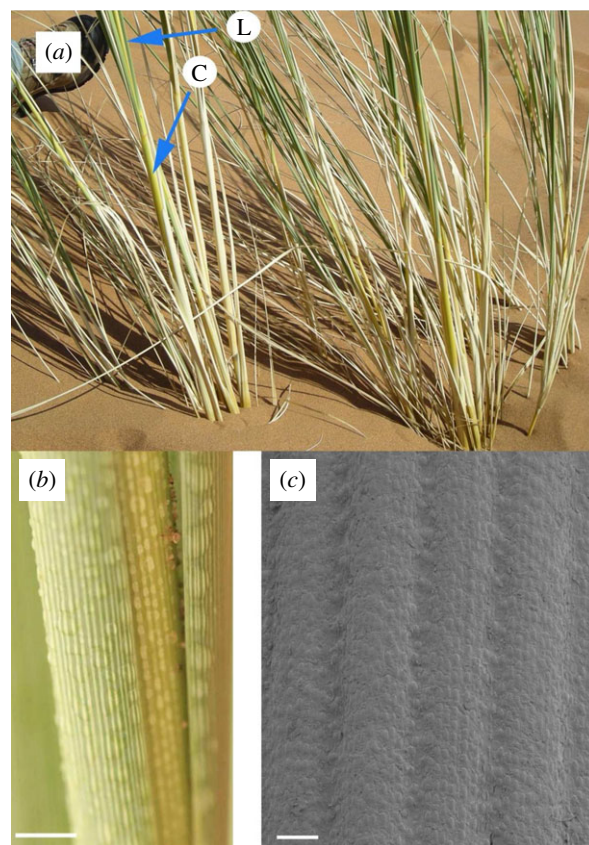
Figure 1. (*a*) Young tussocks of *S. sabulicola* in their natural habitat. C, culms; L, leaves. The culms are tightly enveloped by involute leaves that end in acute tips. (*b*) Drops on involute leaves of *S. sabulicola* after a fog event. The striations correspond to the grooves within the surface. The droplets are sitting on the abaxial (i.e. lower) leaf sides that became the external sides because of the involute state. (*c*) SEM image of the abaxial leaf surface of *S. sabulicola*. (*b*) Scale bar, 1000 μm; (*c*) scale bar, 100 μm. (Online version in colour.)

2.3. Measurements of the contact angle

Contact angle was measured with a DCAT 11 tensiometer (DataPhysics Instruments, Filderstadt, Germany) which is ideal for determining the wettability of cylindrical objects with a strong curvature and a high length to diameter ratio. The sample is slowly immersed into a defined liquid, up to a depth of 5 mm, with the long axis perpendicular to the surface of the liquid. During immersion, the advancing contact angle develops. Then the sample is pulled out, again slowly, with the liquid forming a meniscus at the sample, according to the receding contact angle. This measurement procedure is based upon the Wilhelmy Slide Method [18]. During immersion and extraction, the weight change of the sample is monitored, reflecting the force F caused by the wetting. The contact angle θ can be calculated from F, the perimeter u of the sample and the surface tension γ of the liquid according to

$$\cos \theta = \frac{F}{\gamma u}. \qquad (2.1)$$

2.4. Fog chamber experiments

Native culms of *S. sabulicola* were exposed to an artificial fog stream, produced by the air humidifier Burg

Hebor BH 850E Aquastar, 230 V, 50 Hz, 50 W (Hebor, 1027 Lonay, Switzerland). Water output of the humidifier was $111 \, \text{mm}^3 \, \text{s}^{-1}$. This device produced fog droplets that are comparable in size with natural fog. The velocity of the fog stream was $0.9 \, \text{m s}^{-1}$, which is in the range of the air movement at fog events at the study site in the Namib Desert [16]. During the experiments, room temperature and relative humidity amounted to $12-15°C$ and $70-80\%$, respectively. The orientation angle of the culms was varied from vertical to horizontal positions. Drop behaviour was studied by direct observation and was documented by a camera CANON EOS 450D with a SIGMA 105 Macro objective, and also recorded by a Canon IXUS 75 mounted on a Zeiss binocular under a magnification of 40X. Additionally, the behaviour of droplets on artificial objects, synthetic fibres (see below) and nylon broom bristles exposed to the same fog stream was recorded by the Canon IXUS 75, with the same magnification as above.

2.5. Droplet behaviour on man-made fibres

In order to identify the surface characteristics that are responsible for the droplet behaviour on the surface of *S. sabulicola* leaves, a man-made fibre with a similar surface structure as found in *S. sabulicola* was also tested in the fog chamber. Yarns made from polyester (PET) and polyamide (PA6) were used for the analysis [19]. For the structured fibre, the surface characteristics were reproduced on a PA6 monofilament, a single endless synthetic fibre with a diameter of about $250 \, \mu\text{m}$ (for details of structure see §3.3). To obtain a filament with longitudinal grooves, the polymer was transported by a spinning pump through a spinneret that showed four grooves parallel to its longitudinal axis and therefore, a so called quadrilobal cross section resulted. To remove any oil and dirt from the monofilament, it was washed with the tensid Kiralon OLP at a temperature of $70°C$. Additionally, a round filament was used for comparison reasons.

2.6. Visualization of fog droplets by cryo-scanning electron microscopy

Pieces of *S. sabulicola* were mounted on a sample holder using TissueTek OCT compound (Sakura, Finetek Europe, Zoeterwoude, The Netherlands). The samples were then exposed to the fog airstream (as described above) at time intervals of 5, 10 and 20 s and then immediately frozen in liquid nitrogen in a slushing chamber (vacuum 10^{-1} Pa). After freezing, the samples were immediately transferred to the cooled $(-140°C)$ preparation chamber of the cryo-SEM, a Hitachi S-4800 (Hitachi High-Technologies Corp., Tokyo, Japan) equipped with a GATAN ALTO-2500 cryopreparation system (Gatan Inc., Abingdon, UK). The samples were then sputtered with gold–palladium (6 nm) and examined in the cryo-SEM at 3 kV accelerating voltage and $-120°C$ temperature.
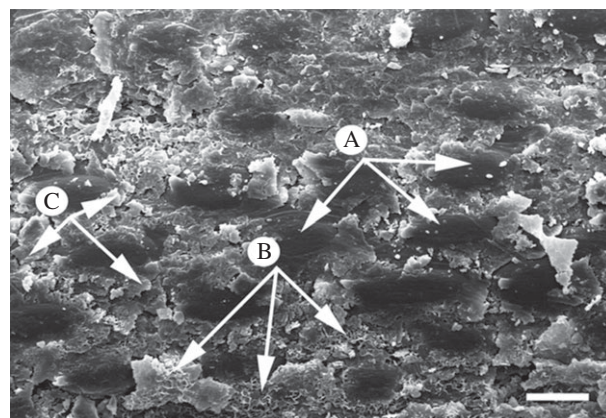
Figure 2. SEM image of the surface of *S. sabulicola*, featuring (A) prickle hairs, (B) putative wax platelets with microcrystalline structure and (C) putative wax platelets without microcrystalline structure. Scale bar, $20 \, \mu\text{m}$.

3. RESULTS

3.1. Surface structure of leaves of S. sabulicola

A conspicuous feature of the leaves are—besides their acute tips and rigid character—the existence of distinct longitudinal ridges and grooves (figure 1*b,c*). The ridges have a diameter of about $100-150 \, \mu\text{m}$ and the grooves have a diameter of about $30-80 \, \mu\text{m}$ (figure 1*c*). The surface is rough and densely packed with silica bodies, amorphous silica within epidermal cells, and prickle hairs as is typical for many grasses [20,21]. The oval prickle hairs are oriented with their longitudinal axis parallel to the longitudinal axis of the leaves and therefore, parallel to the grooves (figure 2). The prickle hairs are positioned within the cuticle, the wax layer covering the leaf. The cuticle has an irregular structure (figure 2) and appears to contain wax platelets. Several wax sublayers may be present. The platelet-like structures possibly result at least partially from sand abrasion occurring in the desert environment. It is also possible that some of these structures represent salt particles that were deposited on the plant surface in the form of aerosols. Such airborne particles are almost indistinguishable from irregular surface waxes [22].

By using AFM, the roughness of the surface was measured as the ratio of actual surface area to the projected surface area. The roughness of the native surface of *S. sabulicola* amounts to about 1.18 (see electronic supplementary material for an example of an AFM image).

3.2. Apparent contact angle of leaves of S. sabulicola

The apparent advancing contact angle for water on leaves of *S. sabulicola* is $\theta_a = 98° \pm 5°$ (i.e. mean value $\pm$ s.d.: $n = 10$) and the receding angle $\theta_r = 56° \pm 9°$ $(n = 9)$. The mean of both values gives by convention the apparent angle $\theta = 77°$. The leaf of *S. sabulicola* is therefore basically hydrophilic, with slight hydrophobicity only in the case of the advancing angle. This conforms to the shape of droplets

Figure 3. Side view of droplets on leaves of *S. sabulicola*, showing the difference between advancing and receding contact angle. (Online version in colour.)

Figure 4. (*a*) Horizontally oriented *S. sabulicola*, after exposure to a fog stream. On this specimen, particularly few widely spaced droplets appear on the surface. (*b*) A broom bristle (nylon), exposed to a fog stream, also horizontally oriented. Numerous closely spaced droplets develop. (Online version in colour.)

sitting on the surface of the leaves (figure 3). The difference between the advancing and receding angle is about $\theta_{a-r} = 43°$.

3.3. Fog chamber experiments

As was already observed under natural conditions, droplets appear along the surface of *S. sabulicola* leaves after exposure to an artificial fog stream. Closer inspection of the droplet formation process shows that small droplets are preferentially located along the furrows (figure 1*b*). The droplets increase in size by further fog collection and coalescence. Once a droplet attains a critical size, it rolls straight down the culm taking with it all the smaller droplets still clinging to the surface (see electronic supplementary material). If the plants are tilted from the vertical position, droplets still run straight down the leaf surface without detaching. The guided downslide of droplets occurs until leaves attain an almost horizontal position. Detachment is observed only for angles smaller than 15° with respect to a horizontal position.

Synthetic cylindrical objects (PET fibres with circular cross section and nylon broom bristles) exposed to artificial fog behave completely different. Here, the numerous droplets formed along the axis are always more closely spaced than on leaves of *S. sabulicola* (figure 4*a,b*). They then detach in an irregular pattern,

depending on which of the droplets gain a critical size by fog particle capture and coalescence with adjacent droplets. Furthermore, the fog-collection rate of *S. sabulicola* (per area) is about 10 per cent higher than in nylon bristles of the same diameter (nylon bristle $265 \pm 23\,\mathrm{mm^3\,m^{-2}\,s^{-1}}$, $n = 37$; *S. sabulicola* $289 \pm 62\,\mathrm{mm^3\,m^{-2}\,s^{-1}}$, $n = 24$). The difference between both rates is significant (p-value $< 10^{-3}$, $t = 4.04$; two-sample t-test, Systat 12.00.08). The higher collection rate of the plant is probably because of its rough surface as roughness is known to promote particle capture [23].

Based on the observed differences between the nylon object and *S. sabulicola*, we assumed that surface properties of the plant are responsible for the different behaviour of droplets. A synthetic fibre showing longitudinal grooves was then exposed to a fog stream, and the formation and behaviour of droplets upon its surfaces was observed. The used PA6 filament with its four grooves parallel to the longitudinal axis shows a lobed appearance in cross section (figure 5). The maximum width (from lobe ridge to opposite lobe ridge) is 250 μm and the minimum width (from lobe bottom to the opposite lobe bottom) is about 150 μm. The depth of one groove is therefore about 50 μm. The grooves have a curved outline (figure 5). The fibre will be termed quadrilobal filament (QF) throughout the rest of the text. The contact angles of QF are $\theta_a = 54° \pm 2°$ and $\theta_r = 41° \pm 1°$, with a difference of
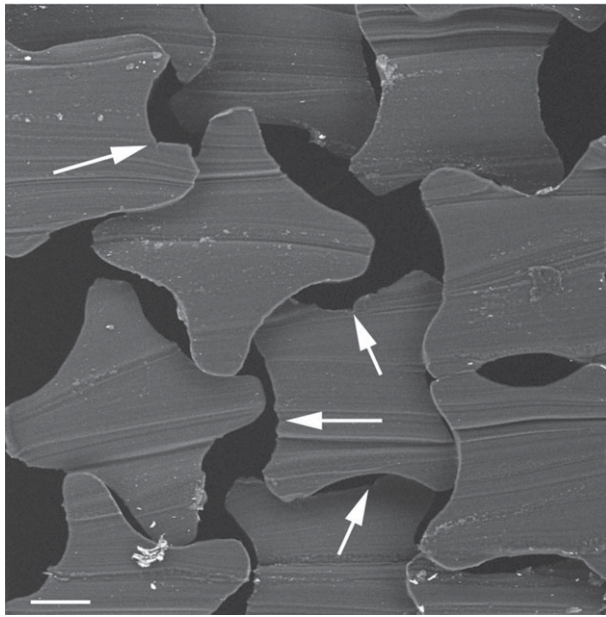
Figure 5. SEM picture of a bundle of quadrilobal PA6 monofilaments, in cross section. Surface irregularities that may serve as pinning sites are marked with white arrows. Scale bar, 50 μm.
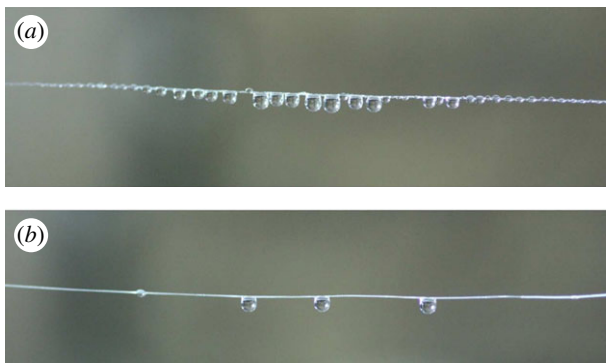
Figure 6. (*a*) Drops on a rounded and (*b*) quadrilobal monofilament. (Online version in colour.)

$\theta_{a-r} = 13°$ between both. For a better examination of the influence of the quadrilobal cross section, a round filament of PET with a similar contact angle as the quadrilobal yarn was used. This round monofilament has a contact angle of $\theta_a = 58° \pm 4°$ and $\theta_r = 35° \pm 3°$. Plane PET foils show a contact angle of about 70° [24,25].

If QF and the round fibre are exposed to a fog stream, droplet behaviour differs fundamentally between both (figure 6*a,b*). Tightly adjacent droplets form along the round filament, whereas very few visible droplets develop on QF (figure 6). This behaviour is for QF almost independent of orientation angle. Drops slide and do not fall off even under low angles of less than 10° to the horizontal position. Sliding droplets take with them all other droplets along their way and the process of droplet formation and growth starts anew. For QF, it can be observed—upon closer inspection—that between the few large growing droplets, very small droplets occur and disappear within the

grooves (see electronic supplementary material). The shapes of the droplets tend to attain the 'clamshell' state for both fibres, probably mainly owing to the contact angle [26]. In this state, droplets do not engulf the fibre completely, but are only attached sideways.

From these observations on the leaves of *S. sabulicola* and the various synthetic objects, it was assumed that (i) fog particles that usually have a diameter of a up to a few 10 μm tend to coalesce inside the furrows of the grooves and (ii) that a flow develops inside the furrows of the grooves which feeds larger droplets clinging to the surface at locations of high pinning. Studies using cryo-SEM were conducted in order to obtain more information on the behaviour of the fog particles once they hit the leaf surface.

3.4. Cryo-scanning electron microscopy studies of microdroplets

Fog droplets were visible as web-like structures upon the leaf surface (figure 7*a–c*). These structures very probably result from partial evaporation of the tiny droplets inside the sample chamber and the addition of the sputter coating layer to the evaporating droplet and its remains. That the web-like structures in fact represent droplets are demonstrated by treating a glass slide in the same manner: glass slides were sprayed with water droplets, and then subsequently frozen in the slushing chamber, rapidly transferred to the cryo-SEM and sputtered. The glass slides in the cryo-SEM were covered with the same structures as could be observed upon the leaf surfaces (figure 7*d*). Droplets detected on the leaf surfaces were usually not smaller than about 14 μm in diameter, and it is possible that smaller droplets evaporated totally either during transfer into the slushing chamber or when sublimated inside the cryo-SEM sample chamber before sputtering.

After 5 s of exposure to the fog stream, droplets are small (figure 7*a*). Many of these droplets are located within or close to the grooves (figure 7*a*). With increasing exposure time to the fog stream, larger droplets appear which are very likely the result of coalescence of several fog droplets (figure 7*b,c*). On several occasions, structures can be detected that appear to represent coalescing droplets (figure 7*b*). In these cases, several rounded structures show merging borders. Also, more extended film-like layers appear after 20 s of exposure (figure 7*c*). These often cover several grooves and ridges. Usually, filaments extend from the larger structures along the grooves (figure 7*c*; see also additional images in the electronic supplementary material).

3.5. Model of surface roughness and droplet sticking

Conditions for droplet downslide along the leaf and droplet detachment from the leaf can be found by comparing the tangential and normal components of gravity forces and surface tension. If (i) the shape of the droplet does not deviate too much from a segment of a sphere and (ii) the contact area between the droplet and leaf is approximately flat, geometric considerations imply that the downslide of the droplet is initiated
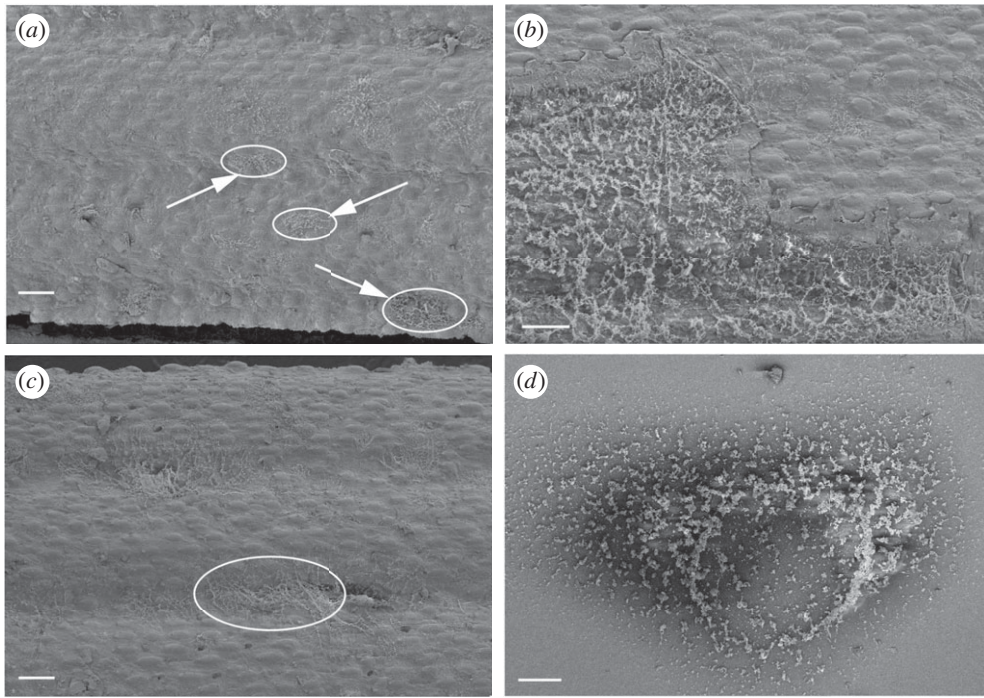
Figure 7. Cryo-SEM pictures of fog droplets upon *S. sabulicola* after different times of exposure to a fog stream (a–c), and upon a glass slide (d). After cryo-SEM preparations, web-like remnants are left by the droplets. (a) Exposure time: 5 s. Some fog droplets are marked by white arrows and additionally highlighted by white elliptic frames. (b) Exposure time: 10 s. One droplet is highlighted by a white elliptic frame. (c) Exposure time: 20 s. (d) Remnants of a water droplet from a sprayer on a glass slide. Scale bars, 50 µm.

when the tangential component of gravity exceeds the tangential component of the surface tension:

$$F_{g,t} \geq F_{\sigma,t}, \tag{3.1}$$

where

$$F_{g,t} = \rho g V \sin\alpha \tag{3.2}$$

and

$$F_{\sigma,t} = k\sigma s(\cos\theta_r - \cos\theta_a). \tag{3.3}$$

Detachment of the droplet occurs when a similar condition for the normal force components holds:

$$F_{g,n} \geq F_{\sigma,n} \tag{3.4}$$

with

$$F_{g,n} = \rho g V \cos\alpha \tag{3.5}$$

and

$$F_{\sigma,n} = \frac{\pi}{2} k\sigma s(\sin\theta_r + \sin\theta_a). \tag{3.6}$$

In the above expression, α denotes the inclination of the leaf with respect to the horizontal axis (cf. figure 8), g the gravitational acceleration, ρ the density of water, V the droplet's volume, s the radius of the droplet's contact circle with the leaf and the constant parameter, k, whose exact value is debated, but values between $\pi/4$ and 2 are commonly considered as acceptable (in what follows, we assume $k = 2$). (A detailed derivation of relations (3.1) through (3.6) has been given elsewhere by Konrad *et al.* [27].) Inspection of the relations

(3.1) and (3.4) shows that the droplet will overcome pinning by (i) a higher tilting angle α or (ii) a larger droplet volume V. Thus, a droplet can detach from the leaf and fall down, it can slide towards the ground along the leaf or it can remain where it is ('persistence'). Conditions (3.1) and (3.4) (for details, see Konrad *et al.* [27]) lead to quantitative expressions for these three options:

$$0° < \alpha < \arctan\left(\frac{2}{\pi}\tan\chi\right) \quad \text{and}$$

$$\begin{cases} V > V_c & \Rightarrow \text{detachment} \\ V < V_c & \Rightarrow \text{persistence} \end{cases}$$

$$\arctan\left(\frac{2}{\pi}\tan\chi\right) < \alpha < 90° \quad \text{and}$$

$$\begin{cases} V > V_s & \Rightarrow \text{downslide} \\ V < V_s & \Rightarrow \text{persistence,} \end{cases} \tag{3.7}$$

where

$$V_s := \frac{\pi l^3}{3}\frac{(1 + \cos\theta)\sin\theta}{\sqrt{2 + \cos\theta}}\sqrt{\left(\frac{2}{\pi}\frac{\sin\chi}{\sin\alpha}\right)^3} \tag{3.8}$$

and

$$V_c := \left\{\frac{\pi l^3}{3}\frac{(1 + \cos\theta)\sin\theta}{\sqrt{2 + \cos\theta}}\right\}\sqrt{\left(\frac{\cos\chi}{\cos\alpha}\right)^3} \tag{3.9}$$

and $\chi := \theta_{a-r}/2$ and $l := \sqrt{6\sigma/\rho g}$.
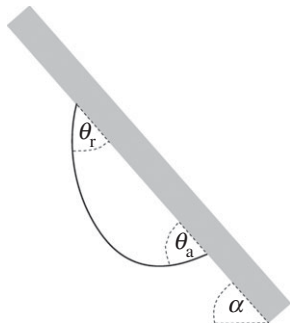
Figure 8. Droplet hanging down from a plane which is inclined against the horizontal axis by an angle α. θ_r and θ_a denote the receding and advancing contact angle, respectively.

Upon insertion of the values $\theta = 77°$ and $\theta_{a-r} = 42°$, related to *S. sabulicola*, schemes (3.7)–(3.9) reduce to

$$0° < \alpha < 13.7° \text{ and} \begin{cases} V > \dfrac{217\,\text{mm}^3}{\sqrt{\cos^3\alpha}} \Rightarrow \text{detachment} \\[3mm] V < \dfrac{217\,\text{mm}^3}{\sqrt{\cos^3\alpha}} \Rightarrow \text{persistence} \end{cases}$$

$$13.7° < \alpha < 90° \text{ and} \begin{cases} V > \dfrac{26\,\text{mm}^3}{\sqrt{\sin^3\alpha}} \Rightarrow \text{downslide} \\[3mm] V < \dfrac{26\,\text{mm}^3}{\sqrt{\sin^3\alpha}} \Rightarrow \text{persistence.} \end{cases}$$

As the model is based on the conditions of a flat and smooth surface, it should be considered as a first approximation to the phenomenon, and complete agreement to the real processes cannot be expected. This will be discussed in §4.

4. DISCUSSION

4.1. Surface roughness and droplet sticking

The rough leaf surface of *S. sabulicola* caused by prickle hairs and partially eroded wax platelets lead to a distinct difference between advancing and receding contact angle of the water droplets. This is because a moving droplet tends to become 'pinned' to local surface irregularities, such as roughness or local differences in surface chemistry [28,29]. Pinning leads to a difference between θ_a and θ_r. This difference $\theta_{a-r} := \theta_a - \theta_r$ is termed contact angle hysteresis and results in a difference in Laplace pressure across the droplet that ultimately causes the droplet to stop moving.

Obviously, contact angle hysteresis realized by *S. sabulicola* is the basic condition that makes quite large droplets able to adhere before they start to glide down under low angles (with respect to the horizontal orientation). This is indicated by the agreement between model results (3.10) and fog chamber results on transition from detachment angle to gliding angle and size of gliding droplets. It should be emphasized that the model assumptions include several simplifications. The most important assumptions are that (i) the droplet is shaped as a spherical segment whose flat side adheres to (ii) a flat culm surface (instead of the real cylindrically curved surface). Neither of these

two assumptions holds for *S. sabulicola*: curved surface, local irregularities and grooves are not considered and the attached droplets deviate, in part, highly from spherical shapes.

These simplifications are probably the reason why the calculated result (approx. 220 mm^3) for the volume of detaching droplets is much larger than the observed volume (approx. 30 mm^3) of droplets falling off from the horizontally oriented culms of *S. sabulicola*. The behaviour of hanging droplets might be more strongly influenced by surface irregularities (particularly if the surface is not planar) as the results of an earlier study considering flat leaves agree much better with the model [27]. For the transition between detachment and downslide, model and fog chamber experiments are in good agreement, because downslide started in all observations at angles below 15°. Also the value $V_c \approx 26\,\text{mm}^3$ matches our observations because sliding droplets usually showed volumes of about 20–30 mm^3.

4.2. The role of the grooves

The downslide motion occurs parallel to the grooves which run along the leaves. In fact, liquid movement on such anisotropic surfaces will generally tend to flow parallel to the grooves [1]. This is because pinning is at a maximum for droplet movement perpendicular to grooves and almost absent when parallel to grooves [28]. Liquids can therefore be guided by anisotropic reliefs [1]. Droplets on the surface of *S. sabulicola* are principally in the Wenzel state, that is, the liquid touches the bottom of the grooves and does not rest upon air that is trapped within the grooves, as is the case for the Cassie state. The Wenzel state allows a much higher degree of adhesion than the Cassie state and can also lead to a substantial elongation of the droplet in flow direction [30]. This can also be observed for droplets on *S. sabulicola* leaves. The contact line on such a surface tends to show a wavy appearance [30]. This also happens to be the case for *S. sabulicola* as is visible on the cryo-SEM pictures. Here, 'water filaments' extend beyond the droplet border (figure 7c).

One reason for the Wenzel state of the droplets is the intrinsic contact angle of the surface material itself. The waxes covering the leaf surface are apparently not hydrophobic. This is suggested by the results of the contact angle measurements showing a mean contact angle of about 77°. Also, the flattened shape of the frozen fog droplets sitting upon the surface of *S. sabulicola* in the cryo-SEM indicates a non-hydrophobic surface. Evaporation during preparation of the cryo-SEM samples may shift the contact angle of the droplets upon *S. sabulicola* more towards the receding angle. If, however, microdroplets are dispersed on hydrophobic glass surfaces and observed in the frozen state in the cryo-SEM, their shape is substantially different from microdroplets on hydrophilic glass surfaces (Dagmar Voigt 2009, unpublished data). Droplets on *S. sabulicola* are more similar to droplets on non-hydrophobic glass surfaces. Therefore, we conclude that the surface of *S. sabulicola* is non-hydrophobic at each location, as is also suggested by the contact angle measurements. Plant waxes in fact show various hydrophilic groups that can render them non-

hydrophobic [31] and usually do not show intrinsic contact angles that are higher than 90° [31].

Water repellency is described by the classic Wenzel relation, giving the inter-relationship between surface roughness r, intrinsic contact angle θ_i and apparent contact angle θ as

$$\cos \theta = r \cos \theta_i. \qquad (4.1)$$

According to Wenzel's relation, a rough surface with $r > 1$ and $\theta_i < 90°$ should show apparent contact angles that are smaller than θ_i. This is the case for *S. sabulicola* with a surface area that is 18 per cent higher than the projected surface. Since θ_i is not known exactly for *S. sabulicola*, it cannot be excluded that the surface achieves a decrease in θ when compared with θ_i owing to roughening. It should, however, be emphasized that Wenzel's relation is often not fulfilled in reality.

4.3. Development of large droplets at the grooves

The behaviour of a groove that becomes filled by vapour condensation was studied by Seemann *et al.* [32] and shown to be dependent on the aspect ratio (ratio between depth and width of the groove) and intrinsic contact angle. Fog droplets landing within the grooves will tend to remain preferentially at the groove corners where adjacent droplets will start to coalesce [32]. For an aspect ratio that is typical for the surface grooves of *S. sabulicola* leaves and contact angles that can be expected for leaf waxes, the liquid is confined to the grooves. The study of Seemann *et al.* [32], however, was carried out on a smooth silicon surface structured by photolithographic methods. In contrast, the surface of *S. sabulicola* is highly irregular mainly owing to wax structures, prickle hairs and external particles that are deposited on the surface.

An important parameter for droplet behaviour on rough surfaces such as in *S. sabulicola* is the relation between the size of the roughness and droplet size. For determining θ on rough surfaces, according to (4.1), droplets have to be observed that are much larger than the surface structures. If the droplets are within the range of the structures, then the droplet will change its shape according to local pinning effects. Thus, for droplets that are not larger than the scale of the surface roughness, θ will be dependent on droplet size. For larger droplets, gravity will become substantial. The behaviour of fog droplets on rough surfaces is therefore highly variable as can be observed on the cryo-SEM pictures (figure 7).

This irregular behaviour will lead to different phenomena after fog droplets start to hit the surface of *S. sabulicola*: droplets coalescing inside the grooves can develop a moving liquid filament inside the grooves, but the occurrence of local surface defects may result in local pinning and overspilling of the groove liquid. Furthermore, droplets sitting on the ridges will also coalesce and eventually join with the groove liquid. Surface irregularities that lead to pinning are important for the development of larger droplets because it needs energy for the ridge-based droplets to expand into the groove, perpendicular to the groove axis. Coalescence between droplets on the ridges and the water inside the grooves would be supported by overspilling caused by pinning. The cryo-SEM pictures show configurations of droplets

that appear to represent these different situations (see electronic supplementary material).

4.4. Insights from the monofilament

Observations on the man-made QF support these assumptions. The aspect ratio for this structure amounts to about 0.2, with an intrinsic contact angle of about 50°. According to the results of Seemann *et al.* [32], under these conditions, an increase in the amount of water inside the grooves by coalescence will lead to a moving water front. Principally, a moving water front inside a groove is described by the kinetics of the Washburn law [33,34]. The detailed kinetics is dependent on the orientation of the groove and on the direction of the water flow with respect to gravity [35].

The dynamics of the water on the surface of *S. sabulicola* and QF and the differences between both objects result, however, from the interaction of various phenomena. Firstly, the grooves lead to the development of capillary forces acting on the water inside the grooves. Secondly, Laplace pressure acts upon droplet shape and coalescence. Thirdly, the behaviour of the water on the surfaces is affected by surface roughness leading to pinning phenomena and therefore, to the readiness of the surface to arrest droplets and the maximum size of droplets. Finally, gravity is of substantial importance as it governs the direction of the moving droplets.

In QF, the rapid formation and disappearance of droplets inside the grooves indicate flow of coalescing droplets along the grooves, feeding few stationary droplets. The question remains of what controls the formation and appearance of the stationary droplets. Closer inspection of QF (figure 5) reveals that the surface of the fibre contains surface defects, i.e. local spots of roughness. It is very likely that at these locations flow is stopped and a growing droplet will develop. The rapid growth of these 'trapped droplets' reflects the high velocity of the supplying water front moving inside the grooves. The much higher degree of surface roughness in *S. sabulicola*, compared with QF, will lead to a higher density of trapped droplets, as is in fact observed.

5. CONCLUSIONS

The ability for conducting the collected fog water towards the plant base with a minimum of loss by droplet scattering is therefore because of the combination of two kinds of surface roughnesses: (i) surface irregularities caused by prickle hairs and platelet-like wax structures prevent the premature shedding of droplets that are too small for downslide and (ii) the presence of grooves parallel to the long axis provides for a guided downslide of larger droplets. In fact, grass species growing in the same area, such as *Stipagrostis lutescens*, do not show the rough and grooved surface of *S. sabulicola* (M. Ebner 2008, unpublished data). Guided flow on plants caused by surface properties was studied by Shirtcliffe *et al.* [2], and a combination of hydrophilic channels within a hydrophobic flat surface was proposed. The leaves of *S. sabulicola* are able to achieve directed water flow mainly by relief and surface roughness, without obvious gradients in wettability.

Assigning all these traits exclusively to the selective advantage of fog collection is, however, too simplistic. Prickle hairs are a common feature of grasses as well as a striated appearance of their leaves. Furthermore, water supply is just one of several difficulties that *S. sabulicola* is confronted within its extreme environment. The thick and scaly waxy layer upon the epidermis that very likely contributes to the contact angle hysteresis θ_{a-r}, may also be related to the exposure to the highly abrasive sand-laden wind. Leaves of desert plants are often mechanically very stiff, with a high amount of sclerenchymatous tissue and a thick cuticle. Also the leaf grooves may be involved in mechanical stability of the upright axes that reach considerable height.

Taken by itself, each of the traits that promote fog collection and directed stem flow appears to represent a common feature of desert plants and/or grasses. Nevertheless, the combination of the leaf surface properties promoting stem flow irrigation together with the tall and upright stature lifting the culms into zones of high wind velocity and the shallow root system that is able to rapidly absorb the collected water constitutes a highly efficient natural fog-collecting system. All these traits enable *S. sabulicola* to thrive in a hyperarid environment and to provide shelter and food for numerous other desert organisms.

The results achieved with QF showed that directed conduction of droplets that attach to the object until they reach the ground can be easily obtained with man-made filaments that are longitudinally grooved. Fog collection is a topic of increasing interest in areas with water shortage. In fog collectors, harvested water may be partially lost by droplet scattering or shed before it arrives at the pipes or troughs. Fibres that are devised according to the structure of *S. sabulicola* leaves may contribute to higher fog yields. Fog collection may therefore be one biomimetic application in which the strategy of *S. sabulicola* can be implemented.

REFERENCES

1 Quéré, D. 2008 Wetting and roughness. *Annu. Rev. Mater. Res.* **38**, 71–99. (doi:10.1146/annurev.matsci.38.060407.132434)

2 Shirtcliffe, N. J., McHale, G. & Newton, M. I. 2009 Learning from superhydrophobic plants: the use of hydrophilic areas on superhydrophobic surfaces for droplet control. *Langmuir* **25**, 14 121–14 128. (doi:10.1021/la901557d)

3 Koch, K., Bhushan, B. & Barthlott, W. 2008 Diversity of structure, morphology and wetting of plant surfaces. *Soft Matter* **4**, 1943–1963. (doi:10.1039/b804854a)

4 Barthlott, W. *et al.* 2010 The Salvinia Paradox: superhydrophobic surfaces with hydrophilic pins for air retention under water. *Adv. Mater.* **22**, 2325–2328. (doi:10.1002/adma.200904411)

5 Gorb, E. V. & Gorb, S. N. 2006 Physicochemical properties of functional surfaces in pitchers of the carnivorous plant *Nepenthes alata* Blanco (Nepenthaceae). *Plant Biol.* **8**, 841–848. (doi:10.1055/s-2006-923929)

6 Holder, C. D. 2007 Leaf water repellency of species in Guatemala and Colorado (USA) and its significance to forest hydrology studies. *J. Hydrol.* **336**, 147–154. (doi:10.1016/j.jhydrol.2006.12.018)

7 Ritter, A., Regalado, C. M. & Aschan, G. 2009 Fog reduces transpiration in tree species of the Canarian relict heath-laurel cloud forest (Garajonay National Park, Spain). *Tree Physiol.* **29**, 517–528. (doi:10.1093/treephys/tpn043)

8 Fischer, D. T., Still, C. J. & Williams, A. P. 2008 Significance of summer fog and overcast for drought stress and ecological functioning of coastal California endemic plant species. *J. Biogeogr.* **36**, 783–799. (doi:10.1111/j.1365-2699.2008.02025.x)

9 Dawson, T. E. 1998 Fog in the California redwood forest: ecosystem inputs and use by plants. *Oecologia* **117**, 476–485. (doi:10.1007/s004420050683)

10 Liu, W., Meng, F. R., Zhang, Y., Liu, Y. & Li, H. 2004 Water input from fog drip in the tropical seasonal rain forest of Xishuangbanna, South-West China. *J. Tropic. Ecol.* **20**, 517–524. (doi:10.1017/S0266467404001890)

11 Aboal, J. R., Morales, D., Hernandez, M. & Jimenez, M. S. 1999 The measurement and modelling of the variation of stem-flow in a laurel forest in Tenerife, Canary Islands. *J. Hydrol.* **221**, 161–174. (doi:10.1016/S0022-1694 (99)00086-4)

12 Ingraham, N. L. & Mark, A. F. 2000 Isotopic assessment of the hydrologic importance of fog deposition on tall snow tussock grass on southern New Zealand uplands. *Austral Ecol.* **25**, 402–408. (doi:10.1046/j.1442-9993.2000.01052.x)

13 Seely, M. K., de Vos, M. P. & Louw, G. N. 1977 Fog imbibition, satellite fauna and unusual leaf structure in a Namib Desert dune plant, *Trianthema hereroensis*. *S. Afr. J. Sci.* **73**, 169–172.

14 Hamilton III, W. J., Henschel, J. R. & Seely, M. K. 2003 Fog collection by Namid Desert beetles. *S. Afr. J. Sci.* **99**, 181.

15 Louw, G. N. & Seely, M. K. 1980 Exploitation of fog water by a perennial Namib dune grass, *Stipagrostis sabulicola*. *S. Afr. J. Sci.* **76**, 38–39.

16 Ebner, M., Miranda, T. & Roth-Nebelsick, A. 2011 Efficient fog harvesting by *Stipagrostis sabulicola* (Namib dune bushman grass). *J. Arid Environ.* **75**, 524–531. (doi:10.1016/j.jaridenv.2011.01.004)

17 de Winter, B. 1965 The South African Stipeae and Aristideae (Gramineae) (an anatomical, cytological and taxonomic study). *Bothalia* **8**, 201–404.

18 Adamson, A. W., Gast, A. P. & NetLibrary, I. 1997 *Physical chemistry of surfaces*. New York, NY: Wiley.

19 Sarsour, J., Linke, M. & Planck, H. 2010 Bionic development of textile materials for harvesting water from fog. In *Proc. 5th Int. Conf. Fog, Fog Collection and Dew 2010*, pp. 88–90, 25–30 July 2010. Münster, Germany: C. W. Group.

20 Reimer, E. & Hugo Cota-Sánchez, J. 2007 An SEM survey of the leaf epidermis in danthonioid grasses (Poaceae: Danthonioideae). *Syst. Bot.* **32**, 60–70. (doi:10.1600/036364407780360139)

21 Clark, C. A. & Gould, F. W. 1975 Some epidermal characteristics of paleas of *Dichanthelium*, *Panicum*, and *Echinochloa*. *Am. J. Bot.* **62**, 743–748. (doi:10.2307/2442064)

22 Burkhardt, J. 2010 Hygroscopic particles on leaf surfaces: nutrients or desiccants? *J. Ecol. Monogr.* **80**, 369–399. (doi:10.1890/09-1988.1)

23 Guha, A. 2008 Transport and deposition of particles in turbulent and laminar flow. *Ann. Rev. Fluid Mech.* **40**, 311–341. (doi:10.1146/annurev.fluid.40.111406.102220)

24 Huang, C., Chang, Y. C. & Wu, S. Y. 2010 Contact angle analysis of low-temperature cyclonic atmospheric pressure plasma modified polyethylene terephthalate. *Thin Solid Films* **518**, 3575–3580. (doi:10.1016/j.tsf.2009.11.046)

25 Vassallo, E., Cremona, A., Ghezzi, F. & Ricci, D. 2010 Characterization by optical emission spectroscopy of an oxygen plasma used for improving PET wettability. *Vacuum* **84**, 902–906. (doi:10.1016/j.vacuum.2009.12.008)

26 Eral, H. B., de Ruiter, J., de Ruiter, R., Oh, J. M., Semprebon, C., Brinkmann, M. & Mugele, F. 2011 Drops on functional fibers: from barrels to clamshells and back. *Soft Matter* **7**, 5138–5143. (doi:10.1039/c0sm01403f)

27 Konrad, W., Ebner, M. & Roth-Nebelsick, A. In press. Leaf surface wettability and implications for drop shedding and evaporation from forest canopies. *Pure Appl. Geophys.* (doi:10.1007/s00024-011-0330-2)

28 Cox, R. G. 1983 The spreading of a liquid on a rough solid surface. *J. Fluid Mech.* **131**, 1–26. (doi:10.1017/S0022112083001214)

29 de Gennes, P. G. 1985 Wetting: statics and dynamics. *Rev. Modern Phys.* **57**, 827–863. (doi:10.1103/RevModPhys.57.827)

30 Chung, J. Y., Youngblood, J. P. & Stafford, C. M. 2007 Anisotropic wetting on tunable micro-wrinkled surfaces. *Soft Matter* **3**, 1163–1169. (doi:10.1039/b705112c)

31 Wagner, P., Fürstner, R., Barthlott, W. & Neinhuis, C. 2003 Quantitative assessment to the structural basis of water repellency in natural and technical surfaces. *J. Exp. Bot.* **54**, 1295–1303. (doi:10.1093/jxb/erg127)

32 Seemann, R., Brinkmann, M., Kramer, E. J., Lange, F. F. & Lipowsky, R. 2005 Wetting morphologies at microstructured surfaces. *Proc. Natl Acad. Sci.* **102**, 1848. (doi:10.1073/pnas.0407721102)

33 Washburn, E. W. 1921 The dynamics of capillary flow. *Phys. Rev.* **17**, 273–283. (doi:10.1103/PhysRev.17.273)

34 Rye, R. R., Mann Jr, J. A. & Yost, F. G. 1996 The flow of liquids in surface grooves. *Langmuir* **12**, 555–565. (doi:10.1021/la9500989)

35 Schneider, H., Wistuba, N., Wagner, H.-J., Thürmer, F. & Zimmermann, U. 2000 The impact of lipid distribution, composition and mobility on xylem water refilling of the resurrection plant *Myrothamnus flabellifolia. New Phytologist* **148**, 221–238. (doi:10.1046/j.1469-8137.2000.00759.x)